Journal of Catalysis 284 (2011) 176–183

Contents lists available at SciVerse ScienceDirect

Journal of Catalysis

journal homepage: www.elsevier.com/locate/jcat

Control of chemoselectivity in hydrogenations of substituted nitro- and cyano-aromatics by cluster-derived ruthenium nanocatalysts

Arindam Indra [a], Niladri Maity [a], Prasenjit Maity [a], Sumit Bhaduri [b,*], Goutam Kumar Lahiri [a,*]

[a] Department of Chemistry, Indian Institute of Technology Bombay, Powai, Mumbai 400 076, India
[b] Department of Chemistry, Northwestern University, Evanston, IL 60208, USA

ARTICLE INFO

Article history:
Available online 3 November 2011

Keywords:
Supported catalysts
Clusters
Chemoselectivity
Hydrogenation
Nitro-benzaldehydes
Cyano-benzaldehydes

ABSTRACT

Catalyst precursors **1** and **2**, made by ion-pairing $[H_3Ru_4(CO)_{12}]^-$ with NR_4^+ groups of functionalized MCM-41 and water-soluble poly(diallyldimethylammonium chloride), PDADMAC, respectively, have been evaluated for the chemoselective hydrogenation of nitro- and cyano-benzaldehydes. They are found to be inert toward $-NO_2$ and –CN groups, but active for the reduction of –CHO and >C=C< functionalities. Thus, 3, 4-nitrobenzaldehyde, nitrostyrene, and 3-cyanobenzaldehyde are hydrogenated with full selectivity to the corresponding nitrobenzylalcohols, 1-ethyl-3-nitrobenzene, and 3-cynaobenzylalcohol, respectively. No such chemoselectivity is observed either with PDADMAC-$RuCl_4$ (**3**) or with (5%)Ru-Al_2O_3, where both the functional groups are hydrogenated. Kinetic analyses have been carried out for the hydrogenation of 4-nitrobenzaldehyde with **2**. Existence of an induction time and two competitive equilibriums followed by the product-forming rate-determining step are inferred from the empirically derived rate expression. The kinetic results, structural evidences, and previous work strongly suggest that the observed chemoselectivity is probably a result of the absence of multiple crystal planes, differing in Miller indices, in the cluster-derived catalysts.

© 2011 Elsevier Inc. All rights reserved.

1. Introduction

Transition-metal nanoparticles as catalysts have attracted attention due to the fact that if controlled, their surface structures often give rise to high chemo-, regio-, stereo- and enantioselectivities [1–7]. Among the various recently reported preparative methods, the use of metal carbonyl clusters as precursors of nanoparticles of controlled size and shape is one of the promising approaches for obtaining catalysts of high selectivities [8–11]. In our earlier work, we reported that anionic carbonyl clusters ion-paired on a water-soluble polymer or functionalized silica are effective precursors for nanoparticles of unique chemo- and/or enantioselective reactions [7,12–19]. Very recently, we reported detailed kinetic analysis and STEM studies on the enantioselective hydrogenation of methyl pyruvate with propyl cinchonidium ($CH_2CH_2CH_2NR_3^+$, NR_3 = free base cinchonidine)-functionalized MCM-41-supported $[H_3Ru_4(CO)_{12}]^-$ as the precatalyst [18]. These results showed that in this reaction, the decarbonylated tetrahedral Ru_4 clusters provide uniform crystal faces (1 1 1) and act as the catalytically active intermediates. Also, because unlike similar catalysts made with Pt clusters, the Ru_4 clusters undergo negligible aggregation under the hydrogenation conditions; good enantioselectivity is obtained even with high turnovers.

The work reported in this paper had two main objectives. First, we wanted to find out whether the cluster-derived Ru_4 catalyst would show unusual chemoselectivities in hydrogenation reactions that are of importance in the fine chemical industries. We chose hydrogenations of nitro- and cyano-benzaldehydes as the test reactions. Nitro- and cyano-benzyl alcohols are of considerable industrial interest, because they find use as pharmaceutical, agrochemical, and liquid crystal intermediates, and also for producing monomers of functional polymers. Many reagents and a few catalysts have been reported for accomplishing some of these reactions, but they all have the limitations in generation of solid waste and/or poor catalytic performance [20,21].

Second, we also wanted to achieve these reductions in water rather than in organic solvents. From the environmental and safety point of views, water is a highly desirable solvent [22–24]. However, MCM-41 cannot be used as the support in water due to its poor hydrolytic stability. Therefore, to achieve this objective, we chose poly(diallyldimethylammonium chloride) (PDADMAC), a water-soluble polyelectrolyte, as the support material. In our earlier papers, hydrogenations and oxidations of a variety of substrates using PDADMAC-supported Pt-cluster-derived catalysts have been reported [7,16,17].

* Corresponding authors.
E-mail addresses: s-bhaduri@northwestern.edu (S. Bhaduri), lahiri@chem.iitb.ac.in (G.K. Lahiri).

0021-9517/$ - see front matter © 2011 Elsevier Inc. All rights reserved.
doi:10.1016/j.jcat.2011.09.020

Thus, in this article, we describe results on nitro- and cyano-benzaldehyde hydrogenations and related reactions using PDADMAC and propyltriethylammonium ($CH_2CH_2CH_2NEt_3^+$)-functionalized MCM-41-supported $[H_3Ru_4(CO)_{12}]^-$ as the precatalysts (Scheme 1). Both **1** and **2** have been found to be fully chemoselective and give good turnovers (⩽625) (Scheme 2). The observed chemoselectivity is totally absent in commercially available Ru/Al_2O_3 and water-soluble Ru-catalyst **3** made by in situ hydrogen reduction of $RuCl_3$. Furthermore, the chemoselectivity of the cluster-derived catalysts is exactly opposite to that of other recently reported and specially prepared nanocatalysts, including that of ruthenium [25–27]. These observations underscore the potential of carbonyl clusters for the syntheses of catalysts of unique chemoselectivity.

2. Experimental section

2.1. Materials and instrumentation

All the preparations and manipulations were performed using standard Schlenk techniques under an atmosphere of dinitrogen. Solvents were dried by standard procedures (toluene over Na/benzophenone; methanol over Mg-turnings/iodine), distilled under nitrogen, and used immediately. $Ru_3(CO)_{12}$, poly(diallyldimethylammonium chloride) (20% aqueous solution, molecular weight 100,000–200,000), and (3-nitrobenzaldehyde, 3-nitrostyrene, 1-ethyl-3-nitrobenzene, 1-nitro-2-phenylethylene, 3-ethylaniline) were obtained from Aldrich. The commercial catalyst 5% Ru/Al_2O_3 was purchased from Alfa Aesar. Potassium hydroxide, triethylamine, iodine, methanol, acetone and toluene were obtained from Merck India Limited, Mumbai, India. Double-distilled water was used for the catalytic studies in water. Hydrogen gas cylinder was supplied by BOC India limited, India. Ruthenium trichloride ($RuCl_3 \cdot nH_2O$), Mg-turnings, and sodium were purchased from S. D. Fine Chemicals, Mumbai, India.

Infrared spectra were taken on a Nicolet spectrophotometer with samples prepared either as KBr pellets or in methanol solution. UV–vis spectroscopic studies were performed at 298 K in a Perkin Elmer Lambda 950 spectrophotometer. TEM studies of the catalysts were done using JEOL-JEM-2100F FEG-TEM. The bulk ruthenium content of fresh and used catalysts was determined on an 8440 Plasma Lab ICP-AES instrument. ^1H NMR and ^{13}C NMR spectra in solution were recorded at 300 and 400 MHz Varian FT NMR spectrometer. Solid-state ^1H NMR spectra were obtained on a Bruker DRX 500 NMR spectrometer. GC experiments were performed with Shimadzu-2014 Gas chromatograph using Astec Chiraldex B-DM (50 m × 0.25 mm × 0.12 μm) column from Sigma–Aldrich.

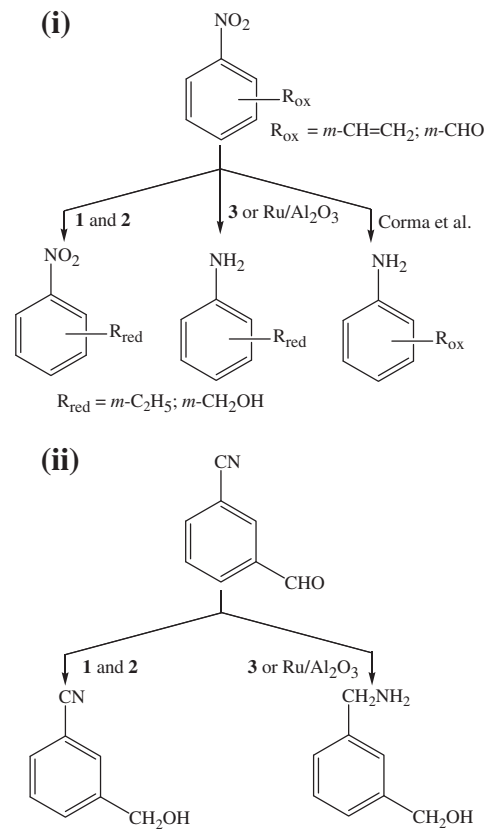

Scheme 2. Product selectivities with **1**, **2**, **3**, and Ru/Al_2O_3.

2.2. Syntheses and characterization of *1–3*

For the synthesis of **1**, triethylamine-modified (3-chloropropyl)trimethoxysilane-functionalized MCM-41 [14,15] (1 g) was added to a 10 mL methanolic solution of $K[H_3Ru_4(CO)_{12}]$ [28] (0.4 g), and it was stirred magnetically at 300 K for 3 h. The solid was filtered off, washed with dry methanol, and dried in vacuum. Analytical data consisted off: 0.4 mmol/g of chloropropyl ammonium (by C, H, N analyses) and ruthenium incorporation: 0.2 mmol/g (by ICP-AES).

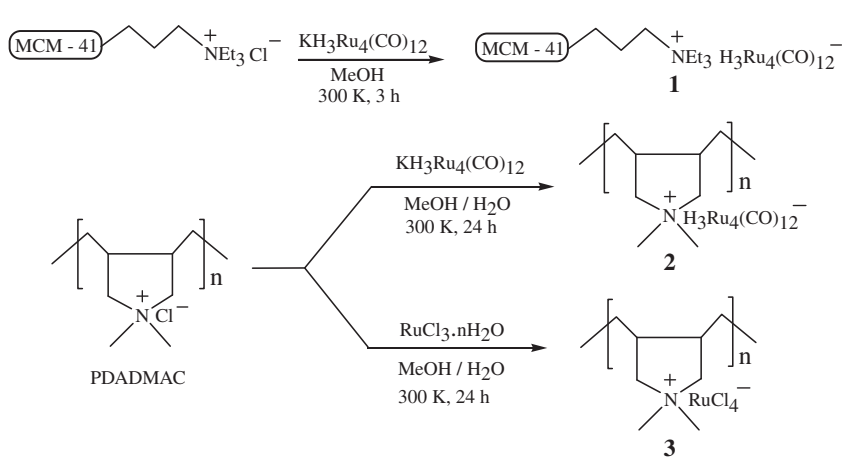

Scheme 1. Synthetic routes for the catalysts **1**, **2**, and **3**.

For the synthesis of **2**, commercially available 20% aqueous solution (2 ml) of PDADMAC [molecular weight 100,000–200,000] was added to a 10 mL methanolic solution of $K[H_3Ru_4(CO)_{12}]$ (0.128 g, 0.16 mmol), and the mixture was stirred at room temperature for 24 h. The solution volume was reduced to 5 mL, and the solid mass was precipitated out using acetone, washed thoroughly with acetone, and dried in vacuum. Ruthenium incorporation: 0.64 mmol/g (by ICP-AES).

For the synthesis of **3**, 20% aqueous solution (3 mL) of PDADMAC [molecular weight 100,000–200,000] was added to a 10 mL aqueous solution of $RuCl_3 \cdot nH_2O$ (100 mg) and stirred at room temperature for 24 h. The volume of the solution was reduced under low pressure, and the solid mass was precipitated out using acetone. The collected residue was washed several times with acetone and dried in vacuum. Ruthenium incorporation: 1.024 mmol/g (by ICP-AES).

2.3. Catalytic, recycling and kinetic experiments

Unless specified otherwise, all hydrogenation reactions were carried out at 353 K in small glass vials placed inside a 200-mL autoclave with vigorous magnetic stirring ($\geqslant$900 RPM). Conversions and selectivities were measured by ^{1}H NMR and gas chromatographic techniques. All hydrogenated products were initially identified by using authentic commercial samples of the expected products.

The recycling experiments with **1** and **2** were carried out at 353 K under 50 and 40 bar H_2 pressure, respectively, with a substrate-to-Ru molar ratio of 283 and 625 in 5 mL of methanol and water, respectively. Recycling experiments with **2** covering five successive batches were also carried out with styrene as the substrate, with a styrene-to-Ru molar ratio of 625 in 5 mL of methanol. Catalyst **1** was filtered off, washed several times with methanol, and used for the second batch. For the reaction with **2**, the product was separated from the aqueous solution by ethyl acetate extraction (2 × 10 mL). The aqueous solution of **2** was then reused. A few recycling experiments were also carried out, where **2** was precipitated from the water solution by the addition of acetone and reused. The results obtained by both these methods of catalyst recovery were comparable.

The kinetic runs with **2** were carried out at 353 K in 5 mL of water in duplicates. For the k_{obs} measurements, calculated amount of **2** was added in the reaction mixture. The glass vial was placed in an autoclave, and a hydrogen pressure in the range of 10–50 bars was applied. Reactions under different hydrogen pressures were studied, and the stirring rate of $\geqslant$900 rpm was found to be adequate for reproducible results. Product and selectivity (%) at different time intervals were determined by ^{1}H NMR. All rates were measured within the conversion range of ~5–40% with $\geqslant$80% data points in the range of 10–25% conversion.

3. Results and discussion

3.1. Syntheses and characterization

Surface functionalization of MCM-41 with propyltrialkylammonium chloride groups ($CH_2CH_2CH_2NR_3^+Cl^-$) (R = Et or cinchonidine) is carried out in two steps, and the detailed synthetic procedures plus characterizations of the functionalized supports have been given in our earlier publications [14,15,19]. Synthesis and characterization of **4**, the cinchonidine analog of **1**, have also been reported by us [19]. Precatalyst **1** is obtained by the same synthetic procedure as that for **4** using $CH_2CH_2CH_2NEt_3^+$-functionalized MCM-41.

The elemental analyses data of **1** show the amine content to be about half of that of **4**. Our earlier work had shown that steric bulks, shapes, and other physico-chemical properties of the amines have observable effects on the degree of incorporation of the NR_3 groups. One of the contributing factors for lower NEt_3 incorporation is its volatility (b.p. 89 °C). The reaction between NEt_3 and MCM-41 functionalized with chloropropyl silane groups is carried out in refluxing toluene, where the concentration of NEt_3 is considerably less than that of cinchonidine. The bulk Ru content in **1** is about twice to that of **4**. The ion pair of $[H_3Ru_4(CO)_{12}]^-$ with $CH_2CH_2CH_2NR_3^+$ is expected to be much smaller and sterically less demanding for NEt_3 rather than cinchonidine. Thus in **1**, the smaller size of the ion-pair probably allows higher loading of the Ru-cluster in the mesopores of the support.

In our earlier publications, BET, IR, XPS, TEM, and STEM data of fresh and used **4** have been reported and discussed at length [18–19]. As the only difference between **1** and **4** is in the identity of NR_3, the characterization data of **1** and **4** are found to be nearly identical and will be discussed only briefly. In BET, 90% of the total pore volume is found to come from pores having radii within the range of 1–2 nm, and the internal surface area contributes more than 90% to the total surface area. IR shows CO vibration bands in approximately the same positions at that of the parent cluster. XPS shows that most of the Ru is present in the zero oxidation state. By TEM in the fresh precatalyst, no Ru-particle could be observed, but STEM (HAADF) shows subnano (~0.5 nm) size particles of the Ru_4 clusters.

Solid-state NMR data of **4** is expected to show the characteristic Ru-H signal, but have not been reported. To provide further support that in freshly prepared **1,** the molecular identity of the cluster is indeed retained, solid-state ^{1}H NMR (MAS) of **1** has also been recorded (Fig. 1a). A metal hydride signal is observed that has a chemical shift ($\delta \sim -17$ ppm) identical with that of the free cluster. On storage under nitrogen and even CO, the inorganic carbonyl IR vibration bands and the metal hydride signal of **1** disappear in $\leqslant$1 h, indicating a change in the ligand environment.

The Ru-content in **2** is ~0.64 mmol/g. Simple calculations show that for the observed Ru-content, ~0.026 cluster anions must be present for every diallyldimethylammonium chloride unit, i.e., every monomer of the support. The molecular weight of the PDADMAC used by us is ~100,000–200,000, which suggests that ~16–32 clusters must be present per polymer molecule.

For **2**, the spectral data (^{1}H and ^{13}C NMR in Fig. 1b and c), IR (Fig. S1, Supplementary information), UV–vis (Fig. S2, Supplementary Information) in solution and TEM (Fig. S3, Supplementary Information) have been recorded. The spectral data show that in the fresh catalyst, the molecular identity of the cluster is retained. In the UV–vis spectrum of $K[H_3Ru_4(CO)_{12}]$, a charge transfer band is observed at ~350 nm. This band is also exhibited by freshly prepared **2**. In IR, broad inorganic carbonyl vibration bands are observed. The Ru-H signal at ~δ, −17 ppm and the CO ligands ~δ, 197 ppm can also be seen by ^{1}H and ^{13}C NMR, respectively (Fig. 1). The ligand environment of **2** is not indefinitely stable, but compared to **1** the characteristic UV–vis, IR, and NMR signals are retained for a much longer time ($\leqslant$48 h).

Attempts to record STEM images of **2** have been unsuccessful. However, HRTEM images of fresh and used **2** show nanoparticles ranging in sizes from ~2 to 5 nm with about 40% being ~3 nm (Fig. S3, Supplementary Information). As TEM is known to modify small metal clusters on inorganic supports during the imaging process, it is possible that agglomeration of the Ru_4 clusters is brought about [29] by TEM. A more likely explanation, however, is that the flexible polymer undergoes folding, enabling weak interactions between regions where the cluster anions are located. The thermodynamic driving force for such interaction is probably the formation of energetically favored quasi-micelle-type

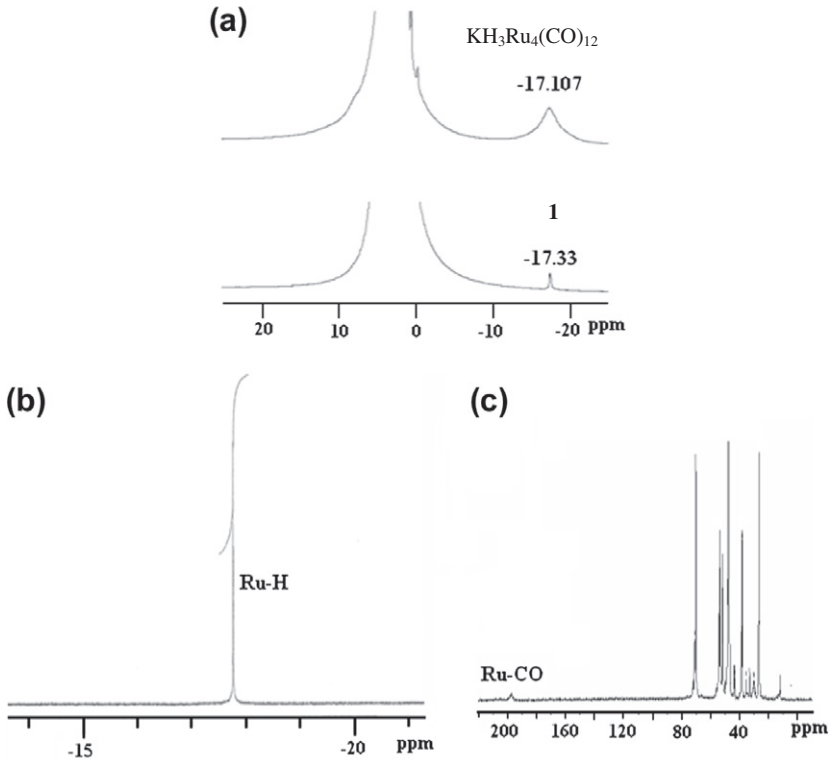

Fig. 1. (a) ^{1}H (MAS) NMR of $[H_3Ru_4(CO)_{12}]^-$ and **1**; (b) and (c) ^{1}H and ^{13}C NMR spectra of catalyst **2** in CD_3OD, respectively.

agglomerates. The support for this explanation comes from the following considerations. First, as mentioned earlier, the presence of discrete Ru_4 clusters in **1** and **4** has been established by STEM (HAADF) [18]. As will be seen later, **1** and **2** have remarkably similar and unique chemoselectivity, indicating that in **1** and **2**, the cluster-derived catalytically active species are probably similar. The main difference between **1** and **2** is that, for the former, the support MCM-41 is insoluble and non-flexible. Second, in solution, reversible agglomerations of PDADMAC-supported platinum clusters were established by spectrophotometric monitoring [16,17]. In this context, it is important to point out that spectrophotometric monitoring has been successfully used by Wang et al. to extract kinetic and other information about the cluster formation process of Pd, Au, and Ag in situ [30]. Finally, it may be noted that the observed sizes of the nanoparticles indicate that in each of them, there are ~4 to 10 cluster units ($Ru_4 \sim 0.5$ nm).

3.2. Selectivity and other related studies

As already mentioned, investigation of whether or not **1** and **2** possess unique chemoselectivity has been one of the primary motivations for this work. For this reason, the selectivity aspect was studied first. The comparative selectivity data of **1**–**3** and commercial Ru(5%)/Al_2O_3 as hydrogenation catalysts for aromatic substrates with functional groups such as >C=C<, –CHO, $-NO_2$, and –CN are given in Table 1. The reactivity of **1** and **2** toward a single functional group has been evaluated by using monofunctional aromatic substrates (Experiment sets 1–4, Table 1). With styrene and benzaldehyde **1** and **2** are found to be active for the reduction of >C=C< and –CHO groups (turnovers ⩾610), but with nitrobenzene and benzonitrile, no reduction of the $-NO_2$ and –CN functionalities are observed. In contrast, control experiments showed **3** and Ru/Al_2O_3 (5%) to be active for the hydrogenation of nitrobenzene and benzonitrile. In this context, it may be noted that by using a mixture of H_2 and CO as reductant and a similar ruthenium cluster, $[Ru_4H_2(CO)_{12}]^{2-}$, as the homogeneous precatalyst, Wada et al. had studied the reduction of benzaldehyde and nitrobenzene [31]. They found this cluster to be an effective precatalyst for the reduction of nitrobenzene, but not benzaldehyde, i.e., the observed selectivity was opposite to that of **1** and **2**. We have not studied the effect of the presence of CO on the catalytic performances of **1** and **2**, as it would likely to have an effect on the induction time associated with the creation of coordinative unsaturation (see later).

Based on these observations, the selectivities of all the catalysts toward aromatic substrates with dual functionalities were evaluated. With R-C_6H_4–NO_2 (R = *m*-CH = CH_2 or *m*-CHO) as substrates (Experiment sets 5 and 6, Table 1), **1** and **2** reduced *only* the "R" group with 100% selectivity (turnovers ⩾220). In contrast, both **3** and Ru/Al_2O_3 reduced *both* "R" and the nitro groups (see Scheme 2). Selective hydrogenation of the double bond in 1-nitro-2-phenyl ethylene is also effected by (Experiment set 7) **1** and **2** (turnovers >55). Here, again **3** and Ru/Al_2O_3 do not show any selectivity, and the only product is 1-amino-2-phenyl ethane. It may be noted that in this substrate, the $-NO_2$ group is closer to the olefinic double bond than in *m*-nitrostyrene and attached to a non-aromatic sp^2-hybridized carbon. Both these factors have no observable effect on the selectivity of **1** and **2**, but a drop in the turnovers is observed (see later). Similar differences in the selectivity of **1** and **2** on the one hand and **3** and Ru/Al_2O_3 on the other hand are also observed, with *m*-CHO–C_6H_4–CN as the substrate (Experiment set 8, Table 1). The cluster-derived catalysts hydrogenate *only* the –CHO group, while both the –CHO and the –CN functionalities are hydrogenated by **3** and Ru/Al_2O_3 (Scheme 2). These results clearly show that the carbonyl cluster-derived catalysts have unique chemoselectivity that is totally absent in the $RuCl_3$-derived or the commercial catalyst. It may also be noted that selectivity of **1** and **2** is exactly opposite to that of recently reported nanocatalysts of Liu et al. and Corma et al. [25–27].

For most of the substrates, the turnovers with **2** are more than that with **1**. The only exception is nitrostyrene, where full (~280 turnovers) and 35% (~220 turnovers) conversions are obtained with **1** and **2**, respectively. With 1-nitro-2-phenylethylene, low

Table 1
Selective catalytic reactions[a].

Experiment set	Substrate	Product	Catalyst	(%) Conversion (chemoselectivity)
1	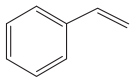	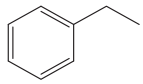	**1** **2**	100(100) 100(100)
2	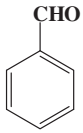	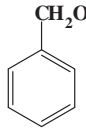	**1** **2**	100(100) 98(100)
3	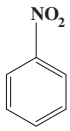	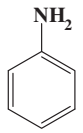	**1** **2**	0 0
4	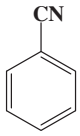	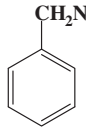	**1** **2**	0 0
5	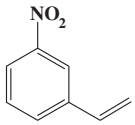	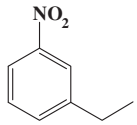	**1** **2** **3** **Ru/Al$_2$O$_3$**	100(100)[b] 35(100) 100(0)[c] 100(0)[c]
6	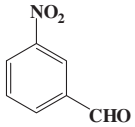	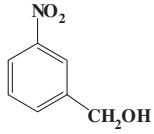	**1** **2** **3** **Ru/Al$_2$O$_3$**	100(100)[b] 55(100) 100(0)[c] 100(0)[c]
7	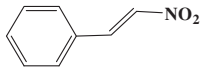	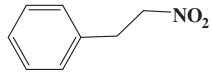	**1** **2** **3** **Ru/Al$_2$O$_3$**	20(100)[b] 15(100) 100(0)[c] 100(0)[c]
8	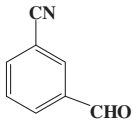	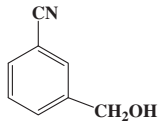	**1** **2** **3** **Ru/Al$_2$O$_3$**	28(100)[b] 46(100) 100(0)[c] 100(0)[c]
9	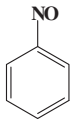	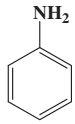	**1** **2**	100(100)[d] 100(100)[d]

[a] *Reaction conditions*: Unless stated otherwise, all reactions were carried out for 4 h at 353 K under 40 bar H_2 pressure with a substrate-to-Ru molar ratio of 625 in MeOH and water (5 mL) for **1** and **2**, respectively.
[b] *Substrate-to-Ru molar ratio*: 283, 12 h, 50 bar H_2 pressure.
[c] Both the functional groups attached to the benzene ring undergo hydrogenation.
[d] Reaction time = 15 min.

turnovers, ~55 and 95, are obtained with both the catalysts. As mentioned earlier, stereo electronic factors are probably the main reason for the low turnovers. For the *meta*-derivatives of nitro- and cyanobezaldehyde, **1** gives ~280 and 80 turnovers, respectively, while with **2**, the corresponding numbers are ~340 and 285.

As the first step in the hydrogenation of nitroaromatics is the formation of the corresponding nitroso derivative, the activity of **1** and **2** toward this reaction has been evaluated [32–34]. Control experiments showed that **1** and **2** are incapable of catalyzing this step, but are active catalysts for the hydrogenation of nitrosobenzene to aniline (Experiment set 9, Table 1). The mechanistic implication of this observation is discussed later. Finally, it may be noted that for *m*-nitro-benzaldehyde, as full conversion is achieved, the calculated turnovers with **1** represents the lowest limit. Thus, for mechanistic investigations and to probe the difference in the activities between **1** and **2** in greater detail, hydrogenation of another isomer of nitro-benzaldehyde was chosen.

With *p*-nitrobenzaldehyde as the substrate, full conversions with **1** and **2**, corresponding to turnovers of 283 and 625, are achieved after 12 and 4 h of reaction, respectively. The effects of reuse on the catalytic performances of **1** and **2** were tested by carrying out two successive batches of *p*-nitro-benzaldehyde hydrogenations. From the time-monitored conversion and selectivity data (Fig. 2), the following conclusions may be drawn.

First, reuse of the catalysts has more of an effect on the product percentage, i.e., turnovers, than on selectivity. Thus, for **1** and **2**, at the end of the second batch, the product percentages are 15% and 37% less than those in the first batch. In contrast, the selectivity of **1** and **2** decreases only by 10% and 1%, respectively. Second, on reuse, there is a decrease in the activities of both the catalysts, but for **2**, the drop in activity is more pronounced. The average turnover frequencies (TOF) may be used as an approximate measure for the activities of the catalysts. The TOF of **1** and **2**, calculated from the slopes of the least-square-fitted straight lines in the turnover

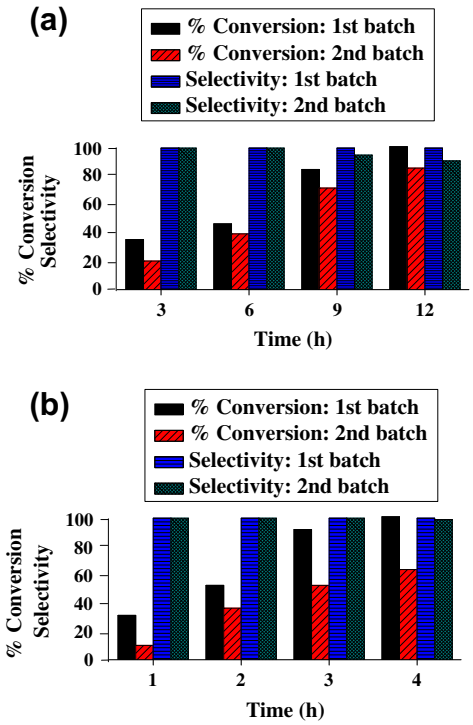

Fig. 2. Time versus conversion (%) and selectivity (%) in two successive batches, (a) by **1** and (b) by **2**.

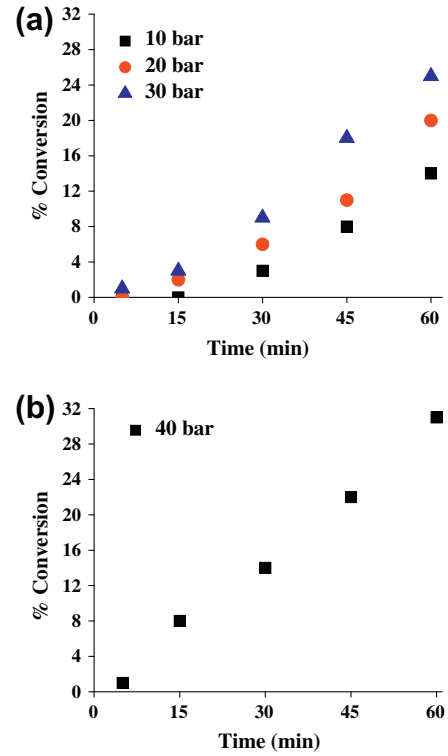

Fig. 3. Plot of time versus conversion of *p*-nitrobenzaldehyde at (a) 10 bar, 20 bar, 30 bar, and (b) 40 bar during hydrogenation with **2**.

versus time plots (Fig. S4, Supplementary Information), for the first batch are ~23.5 and 162.5 h^{-1}, respectively, while for the 2nd batch, they are ~20.9 and 105 h^{-1}. Third, although on recycle, there is a notable drop (~35%) in the TOF of **2**, the change in selectivity is marginal (1%). In contrast, on reuse, the decrease in the TOF and the selectivity of **1**, ~11 and 9%, respectively, are comparable. Repeated measurements of Ru contents after the two batches by ICP-AES show that there is no observable leaching of Ru during the reaction. The reduction in activities on reuse is, therefore, less likely due to Ru loss by leaching. A plausible explanation for these observations based on the mechanism of the reaction and additional experimental evidence to support that the extent of leaching of Ru is negligible, are discussed later.

3.3. Kinetic studies on the hydrogenation of 4-nitrobenzaldehyde by **2**

Kinetic analyses aimed at establishing an empirical rate expression were carried out with **2** rather than **1** for two reasons. First, it is reasonable to assume that at a molecular level, the reaction mechanisms for **1** and **2** will be the same, but due to the use of a solid support, gas–liquid–solid mass transfer effects for **1** may have to be taken into account. Indeed, for the kinetic analyses of enantioselective hydrogenation of methyl pyruvate by **4**, precisely for such effects, simulation techniques based on an unsteady state model were used [18]. Second, as mentioned above, the performance of **2** in terms of activity, selectivity, and the ability to retain selectivity on recycle is superior to that of **1**. Thus, the effects of hydrogen pressure, substrate concentration, and concentration of **2** on the conversion of 4-nitrobenzaldehyde (NBAL) to 4-nitrobenzyl alcohol (NBALC) were studied. From the time-monitored conversion data and rate measurements, the following conclusions may be drawn.

As can be seen from Fig. 3, hydrogenation sets in after an induction time, the length of which depends on the applied pressure. Under a pressure of 10 bars, the induction time is ⩾30 min, while under 40 bars, it is ⩽10 min. In control experiments (Fig. S5, Supplementary Information), when hydrogen is passed through a solution of **2**, complete loss of CO is observed in about ~20 min, and on application of a slight pressure (10 bar), the time taken is much shorter (⩽5 min). The loss of the CO ligands was irreversible, that is, exposure of the decarbonylated material to an atmosphere of carbon monoxide for 24 h did not produce any observable carbonyl bands in the IR. These observations suggest that the induction time is associated with CO loss by the parent cluster with the concomitant in situ formation of the catalytically active intermediate.

Keeping the catalyst and substrate concentration constant if pressure is increased, an increase in turnovers is observed (Fig. 4a). The same plot is also indicative of saturation kinetics with respect to hydrogen pressure. From the [NBAL] versus turnover plots at two different hydrogen pressures (Fig. 4b), it is clear that at a constant pressure, an increase in the substrate concentration lowers the turnovers. These observations indicate the existence of competitive equilibriums, as well as the inhibition of product formation by excess NBAL. Such inhibition would result if both hydrogen and NBAL compete for co-ordination to the unsaturated cluster. In other words, there are two equilibriums, a productive one between **2** and hydrogen, and a non-productive one between **2** and NBAL. Based on the above observations and steady-state approximation, the following kinetic scheme may therefore be proposed.

$$\mathbf{2} + H_2 \overset{K_1}{\rightleftharpoons} \mathbf{2}\text{–}2H \quad \text{(a)}$$

$$\mathbf{2} + \text{NBAL} \overset{K_2}{\rightleftharpoons} \mathbf{2} - \text{NBAL} \quad \text{(b)}$$

$$\mathbf{2}\text{–}2H + \text{NBAL} \overset{k}{\rightarrow} \mathbf{2} + \text{NBALC} \quad \text{(c)}$$

In equilibrium (a), a catalytically active hydride intermediate **2**–2H is produced. A plausible molecular-level formulation of this intermediate is discussed later. However, as shown by (b) in an inhibitory equilibrium, NBAL competes for the active sites and forms a catalytically non-active intermediate **2**-NBAL. In step (c),

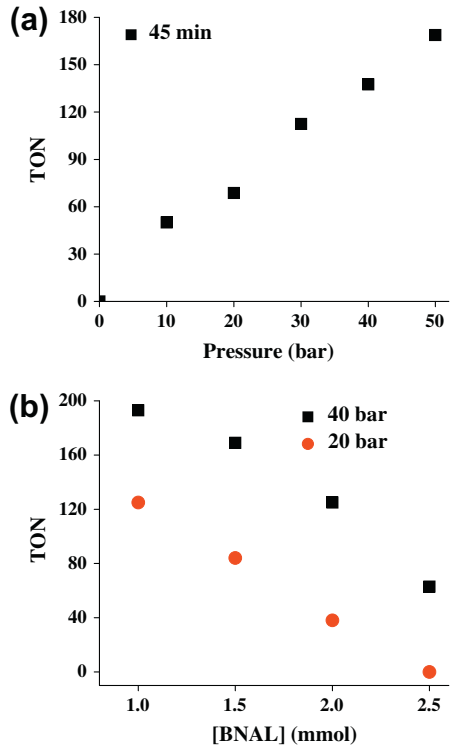

Fig. 4. Plot of (a) change in TON of *p*-nitrobenzaldehyde (1 mmol) with hydrogen pressure at 45 min and (b) TON with concentration of *p*-nitrobenzaldehyde at 20 and 40 bar hydrogen pressure during hydrogenation with **2**.

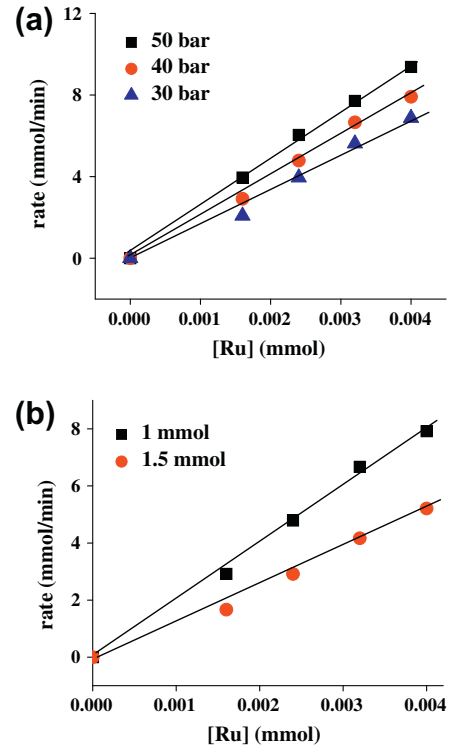

Fig. 5. (a) Plot of rate versus concentration of **2** at 30, 40, and 50 bar hydrogen pressures with 1 mmol substrate and (b) plot of rate versus concentration of **2** at substrate concentration of 1 and 1.5 mmol at 40 bar hydrogen pressure during hydrogenation with **2**.

which is the rate determining step, *p*-nitrobenzyl alcohol is formed from the reaction of **2**–2H and NBAL. The rate expression according to reactions (a)–(c) is as given below.

$$-\frac{d[\mathrm{NBAL}]}{dt} = \frac{d[\mathrm{NBALC}]}{dt} = \frac{k\mathrm{K}_1[\mathbf{2}][\mathrm{H}_2][\mathrm{NBAL}]}{1 + K_1[\mathrm{H}_2] + K_2[\mathrm{NBAL}]}$$

Under pseudo first-order conditions $d[\mathrm{NBALC}]/dt \approx k_{\mathrm{obs}}[\mathbf{2}]$. As can be seen from Fig. 5, good linearity is obtained in the [Ru] versus rate plots at different pressures and NBAL concentrations. This confirms that the reaction is first order with respect to the concentration of Ru. The first-order dependence of the rate on the cluster concentration is consistent with the hypothesis that in the active catalyst, the tetrahedral metal framework is retained intact. The slopes of the straight lines in Fig. 5 provide k_{obs} under different pressures and substrate concentrations, and from the double-reciprocal plots (Fig. S6, Supplementary Information), approximate values of k and K_2/K_1 are found to be ~5000 min^{-1} and 42, respectively.

This reaction scheme is practically identical to the one reported [18] for the enantioselective hydrogenation of methyl pyruvate by **4**. There also a pressure-dependent induction time, a productive equilibrium with H_2, a non-productive one with the substrate, and a product-forming rate-determining step were observed. The only difference between the two kinetic schemes is that for **4**, the equilibrium with H_2 was slow, which resulted in a notably longer induction time. Control experiments showed that hydrogenation of NBAL by **1** also has a longer induction time compared to that of **2**. Thus, it is reasonable to propose that NBAL hydrogenation by **1** and **2** follow the same mechanism, and during catalysis, the decarbonylated clusters of **1** and **2** retain their cluster framework.

Based on the rate expression, the following mechanism for the formation of NBALC may be proposed. Under hydrogen pressure, the carbonyl groups of $[H_3Ru_4(CO)_{12}]^-$ are lost, and hydrogen and NBAL compete for the co-ordinatively unsaturated Ru_4 clusters. There are several reports [35,36], where Rh_4 clusters have shown to be the dominant catalytically active species in hydrogen generation from H_3BNH_3. These findings, the kinetic results, and our earlier work strongly suggest that weakly ligated tetrahedral Ru_4 clusters are relatively stable and catalytically active. Thus, **2**–2H is tentatively formulated as $[Ru_4H_n]^-$ ($n \geqslant 2$) ion-paired with a few of the alkyl ammonium ions of PDADMAC. Excluding the hydrides, the co-ordination sphere of the cluster probably consists of weakly ligated water molecules. The rate expression clearly indicates a transition state that involves Ru_4 clusters, hydride ligands, and NBAL in the rate-determining step. Formation of NBALC from NBAL requires transfer of two hydrogen atoms, of which the transfer of the hydrogen atom to the carbon atom of the carbonyl functionality is probably the rate-determining step. The rate-limiting step is, therefore, proposed to be slow co-ordination by NBAL to $[Ru_4H_n]^-$ followed by fast hydrogen atom transfers.

According to this mechanism, a hypothetical explanation for the unusual chemoselectivity and the effects of recycling on the performance of **1** and **2** may be offered. The nude tetrahedral Ru_4 clusters are expected to provide uniform (111) crystal planes. In methyl pyruvate hydrogenation, the (111) faces of chirally modified nano-Pt have been shown to give higher enantioselectivity than other crystal faces [37]. Our earlier work on the same reaction also suggests that the enantioselectivity of the Ru_4 catalyst originates from the exclusive presence of (111) faces [18]. However, if the reduction of nitrobenzene to nitrosobenzene and the hydrogenation of –CN functionality required crystal planes other than (111), then **1** and **2** would be inert toward these transformations. In **3** and Ru/Al_2O_3, multiple crystal planes are expected to be present. Consequently, $-NO_2$, –CN, and –CHO groups are reduced without any discrimination. The negligible (1%) drop in the chemoselectivity of **2** on reuse is indicative of the fact that under the hydrogenation conditions, the extent of formation of other crystal planes on PDADMC is marginal. In contrast with **1**, the ~10% drop in selectivity probably indicates that on MCM-41, the extent of formation of other crystal faces are more.

The drop in activities of recycled **1** and **2** is probably due the presence of catalytically inactive **1**-NBAL and **2**-NBAL in the recycled catalyst, rather than Ru-loss by leaching. For testing whether or not leaching occurs from a polymer-supported catalyst, many methods, including nanofiltration through an inorganic membrane, have been reported [38]. However, in our case, Ru leaching may be ruled out on the basis of the following two evidences. First, as already mentioned, direct Ru estimation by ICP-AES before and after recycling does not show any Ru leaching. This is found to be the case for both methods of catalyst recovery. Second, remarkably, the drop in activity on recycle is found to be substrate specific. It is observed only with NBAL and not with any other substrate. Thus, hydrogenation of styrene with recycled **2** has been carried out for four successive batches with negligible change in activity.

As mentioned earlier, the kinetic evidence clearly shows the formation of **1**-NBAL and **2**-NBAL in a non-productive inhibitory equilibrium. Before recycling, the separation of **1** and **2,** from the reaction mixture by filtration and solvent extraction or precipitation (see Experimental), is unlikely to remove trace quantities of **1**-NBAL and **2**-NBAL. As K_2/K_1 for **2** is ~42, in the resting state of the catalyst, the amount of **2**-NBAL present is expected to be at least an order more than that of **2**–2H. In other words, the recycled catalyst consists of a mixture of **2**-NBAL, **2**–2H, and **2**, with only the latter two species but not the former contributing to the product-forming pathway. This results in the observed decreases in activity on recycle.

4. Conclusions

In conclusion, we find that $[H_3Ru_4(CO)_{12}]^-$ ion paired with functionalized MCM-41 or water-soluble PDADMAC is an effective precursor for a nanoruthenium catalyst that selectively hydrogenates aldehyde functionality in the presence of nitro- or cyano-group. This chemoselectivity is not observed either with Ru/Al_2O_3(5%), or with $RuCl_3$ supported on poly(diallyldimethylammonium chloride). Kinetic analyses show two competitive equilibriums followed by a rate-determining step. The rate expression, other evidences, and previous reports strongly suggest the involvement of Ru_4 clusters as catalytic intermediates.

Acknowledgments

Financial supports from CSIR, New Delhi, and Reliance Industries Limited, Mumbai, India, are gratefully acknowledged. The suggestions of the reviewers at the revision stage were very helpful.

Appendix A. Supplementary material

Supplementary data associated with this article can be found, in the online version, at doi:10.1016/j.jcat.2011.09.020.

References

[1] G.A. Somorjai, Y. Li, Top. Catal. 53 (2010) 832–847.
[2] C.P. Vinod, Catal. Today 154 (2010) 113–117.
[3] E. Schmidt, W. Kleist, F. Krumeich, T. Mallat, A. Baiker, Chem. Eur. J. 16 (2010) 2181–2192.
[4] C.A. Witham, W. Huang, C.-K. Tsung, J.N. Kuhn, G.A. Somorjai, F.D. Toste, Nat. Chem. 2 (2010) 36–41.
[5] S. Mostafa, F. Behafarid, J.R. Croy, L.K. Ono, L. Li, J.C. Yang, A.I. Frenkel, B.R. Cuenya, J. Am. Chem. Soc. 132 (2010) 15714–15719.
[6] F. Zaera, Acc. Chem. Res. 42 (2009) 1152–1160.
[7] P. Maity, C.S. Gopinath, S. Bhaduri, G.K. Lahiri, Green Chem. 11 (2009) 554–561.
[8] A. Kulkarni, R.J. Lobo-Lapidus, B.C. Gates, Chem. Commun. 46 (2010) 5997–6015.
[9] J.M. Thomas, R. Raja, Top. Catal. 53 (2010) 848–858.
[10] R.D. Adams, E.M. Boswell, B. Captain, A.B. Hungria, P.A. Midgley, R. Raja, J.M. Thomas, Angew. Chem. Int. Ed. 46 (2007) 8182–8185.
[11] J.M. Thomas, R. Raja, D.W. Lewis, Angew. Chem. Int. Ed. 44 (2005) 6456–6482.
[12] S. Bhaduri, V.S. Darshane, K. Sharma, D. Mukesh, J. Chem. Soc., Chem. Commun. (1992) 1738–1740.
[13] H. Paul, S. Bhaduri, G.K. Lahiri, Organometallics 22 (2003) 3019–3021.
[14] S. Basu, H. Paul, C.S. Gopinath, S. Bhaduri, G.K. Lahiri, J. Catal. 229 (2005) 298–302.
[15] S. Basu, M. Mapa, C.S. Gopinath, D. Mukesh, S. Bhaduri, G.K. Lahiri, J. Catal. 239 (2006) 154–161.
[16] P. Maity, S. Basu, S. Bhaduri, G.K. Lahiri, Adv. Synth. Catal. 349 (2007) 1955–1962.
[17] P. Maity, S. Basu, S. Bhaduri, G.K. Lahiri, J. Mol. Catal. A: Chem. 270 (2007) 117–122.
[18] A. Indra, M. Doble, S. Bhaduri, G.K. Lahiri, ACS Catal. 1 (2011) 511–518.
[19] A. Indra, S. Basu, D.G. Kulkarni, C.S. Gopinath, S. Bhaduri, G.K. Lahiri, Appl. Catal. A 344 (2008) 124–130.
[20] M. Kidwai, V. Bansal, A. Saxena, R. Shankar, S. Mozumdar, Tetrahedron Lett. 47 (2006) 4161–4165.
[21] S. Rawale, L.M. Hrihorczuk, W. Wei, J. Zemlicka, J. Med. Chem. 45 (2002) 937–943.
[22] R.A. Sheldon, Green Chem. 9 (2007) 1273–1283.
[23] R.A. Sheldon, Green Chem. 7 (2005) 267–278.
[24] J. Auge, Green Chem. 10 (2008) 225–231.
[25] A. Corma, P. Serna, P. Concepci, J.J. Calvino, J. Am. Chem. Soc. 130 (2008) 8748–8753.
[26] L. Liu, B. Qiao, Z. Chen, J. Zhang, Y. Deng, Chem. Commun. (2009) 653–655.
[27] L. Liu, B. Qiao, Y. Ma, J. Zhang, Y. Deng, Dalton Trans. (2008) 2542–2548.
[28] J.W. Koepke, J.R. Johnson, S.A.R. Knox, H.D. Kaesz, J. Am. Chem. Soc. 97 (1975) 3947–3952.
[29] F. Yang, E. Trufan, R.D. Adams, D.W. Goodman, J. Phys. Chem. C 112 (2008) 14233–14235.
[30] J. Wang, H.F.M. Boelens, M.B. Thathagar, G. Rothenberg, ChemPhysChem 5 (2004) 93–98.
[31] F. Wada, M. Shimuta, T. Matsuda, Bull. Chem. Soc. Jpn. 62 (1989) 2709–2710.
[32] Y. Takenaka, T. Kiyosu, J.-C. Choi, T. Sakakura, H. Yasuda, Green Chem. 11 (2009) 1385–1390.
[33] R.M. Deshpande, A.N. Mahajan, M.M. Diwakar, P.S. Ozarde, R.V. Chaudhari, J. Org. Chem. 69 (2004) 4835–4838.
[34] H.D. Burge, D.J. Collins, B.H. Davis, Ind. Eng. Chem. Prod. Res. Dev. 19 (1980) 389–391.
[35] C.A. Jaska, I.J. Manners, Am. Chem. Soc. 126 (2004) 9776–9785.
[36] R. Rousseau, G.K. Schenter, J.L. Fulton, J.C. Linehan, M.H. Engelhard, T. Autrey, J. Am. Chem. Soc. 131 (2009) 10516–10524.
[37] E. Schmidt, A. Vargas, T. Mallat, A. Baiker, J. Am. Chem. Soc. 131 (2009) 12358–12367.
[38] A.V. Gaikwad, V. Boffa, J.E. ten Elshof, G. Rothenberg, Angew. Chem. Int. Ed. 47 (2008) 5407–5410.